Acid activated smectite clay as pozzolanic supplementary cementitious material

Bamdad Ayati [a,*], Darryl Newport [b], Hong Wong [c], Christopher Cheeseman [c]

[a] *Sustainability Research Institute, University of East London, London E16 2RD, UK*
[b] *Suffolk Sustainability Institute, University of Suffolk, Ipswich IP4 1QJ, UK*
[c] *UKRIC Advanced Infrastructure Materials Laboratory, Department of Civil and Environmental Engineering, Imperial College London, SW7 2BU, UK*

ARTICLE INFO

ABSTRACT

This research has investigated the structural changes and pozzolanic activity produced in acid activated smectite clay. The activation treatment used HCl at different concentrations, using different times and at a range of temperatures. X-ray diffraction, Fourier transform infrared spectroscopy and scanning electron microscopy coupled with energy dispersive X-ray spectroscopy were used to determine the acid dissolution mechanism and characterise the activated clay mineral structure. Acid activation causes dehydroxylation of smectite clay, followed by leaching of octahedral cations. This results in the formation of a silica-rich amorphous phase that exhibits substantial pozzolanic activity compared to the same clay sample that had undergone calcining treatment at 850. The optimum sample was activated for 8 h using 5 M HCl at 90 °C. This was 93 % amorphous. Mortar prisms prepared with 25 % replacement of Portland cement by acid activated smectite produced 93 % compressive strength of plain Portland cement mortar.

1. Introduction

The use of supplementary cementitious materials (SCMs) has been receiving worldwide attention as an option for lowering the CO_2 emissions associated with production of Portland cement (PC). Calcined clays have been extensively researched to form SCMs because clays are geologically abundant, and calcining is a relatively simple, proven and low-cost technology. However, the energy requirement for calcining and the associated CO_2 emission remains a disadvantage of thermally activated clays. Attempts to mechanically activate clay minerals have been successful [1], but these methods also require high energy consumption [2], and the reactivity of the resulting clay minerals is often not comparable with thermally calcined clays [3]. As a result, research that aims to produce SCMs from clays using low-temperature processing methods is of outmost importance.

The reactivity of calcined clays is due to a dehydroxylation reaction that occurs at temperatures between 650 and 900 °C [4]. This produces amorphous aluminosilicates which can react with $Ca(OH)_2$ in cement paste and contribute to strength enhancement [5]. This research explores whether dehydroxylation and amorphization can be achieved by acid treatment as protons penetrate the clay mineral layers and attacks the structural -OH. Previous research has shown that acid treatment releases the central atom from octahedral sites and removes Al from tetrahedral sheets, resulting in the gradual transformation of tetrahedral sheets into a poorly ordered SiO_2 framework [6]. The acid activation also increases the specific surface area (SSA) due to partial destruction of the clay mineral layered structure [7]. Therefore the final reaction product of various acid activated clay minerals can be amorphous, porous, protonated and hydrated silica [8]. This resembles the structure of reactive calcined clays and thus the pozzolanic activity of acid activated clay minerals needs investigation.

The effect of acid activation has been investigated on various clay minerals such as kaolinite, illite and sepiolite [9]. However, the term 'acid-activated clays' has been mainly used for partly dissolved bentonites and acid-activated bentonite has been a standard product for many decades [10]. The dominant mineral phase in bentonite is smectite, a 2:1 hydrous phyllosilicate with octahedral sheets 'sandwiched' between two tetrahedral sheets. Exchangeable interlayer cations such as Na^+, Ca^{2+}, Mg^{2+} and H^+ provide a large chemically active surface area [11]. Acid activated bentonites are widely used as catalysts in applications such as oil discolouration and landfill leachate treatment, where an optimal porosity to achieve maximum adsorption properties is desired [12]. Acid treatments have been extensively studied to improve the absorbency and catalytic properties of smectite clays [13,14]. However,

---

Table 1
Mineral composition calculated through XRD Rietveld analysis and XRF oxide composition of the clay sample and PFA.

	Clay[a]	PFA
Phase composition (wt%)		
Montmorillonite	73.3	–
Hematite	16.6	–
Magnesioferrite	6.6	
Calcite	1.8	–
Quartz	1.6	11.5
Mullite	–	13.1
Amorphous	–	75.4
XRF composition (wt%)		
SiO$_2$	41.84	58.05
Al$_2$O$_3$	15.52	20.35
Fe$_2$O$_3$	13.80	8.90
CaO	3.84	2.84
MgO	2.99	1.73
K$_2$O	0.12	1.88
Na$_2$O	0.04	2.31
TiO$_2$	1.90	0.89
LOI[b]	14.7	1.78

[a] Rietveld quantitative analysis of crystalline phases in the clay sample.
[b] Loss on ignition.

no research has focused on the potential of acid-activated smectite (AAS) clays to act as pozzolanic materials and be used as low-carbon SCMs in concrete.

This paper explores, for the first time, the pozzolanic activity of AAS clays. Changes in the chemical composition, crystal structure and amorphous content of smectite clay subjected to acid treatment were determined using X-ray diffraction (XRD), Fourier Transformed Infra-Red (FTIR) spectroscopy and scanning electron microscopy. The performance of acid-activated smectite clay in a blended cement system was compared with that of cement paste and mortar containing pulverised fuel ash (PFA).

2. Material and methods

2.1. Materials

A sample of smectite-rich London clay was obtained from a clay deposit site (Tarmac Cement Ltd). CEM I 52,5N Portland cement (Blue Circle-ProCem) and PFA (Cementos Tudela Veguin, SAU) were used in the blended systems. To compare acid and thermal activation treatments, a calcined sample of the smectite clay was prepared at 850 °C in an electric furnace with 1 h of dwell time. The chemical composition and mineralogy of the materials were determined using X-ray fluorescence (XRF) and XRD, and the data is given in Tables 1 and 2 respectively. The crystalline phases in the clay sample were montmorillonite (73.3 %), hematite (16.6 %), magnesioferrite (6.6 %), with minor quantities of calcite and quartz.

2.2. Acid activation

Acid activation treatment is usually conducted with 0.5-2 N HCl or H$_2$SO$_4$ for 3–30 min to avoid a complete decomposition of clay minerals and the output solid often contains substantial amounts of parent minerals [8,15]. Since smectites have minimal pozzolanic activity, the intensity of acid treatment was increased until collapse of the clay mineral structure was observed. The as-received clay sample was dried at 105 °C to a constant weight and ball milled to give a 45 μm residue of <50 % prior to the acid treatment. The acid treatment was performed on batches of 10 g of clay with HCl at a liquid to solid (L/S) ratio of 5 ml/g. Table 3 shows the acid treatment conditions used in this study. Variables include treatment duration (1 h to 21 days), temperature (20 °C, 90 °C), acid concentration and agitation. Acid treatment at 90 °C was conducted on a magnetic stirrer and under reflux to minimise the liquid loss. After treatment the suspension was centrifuged at 2500 rpm for 3 min to separate the solids. The solid fractions were washed with de-ionized water at 10–15 l/kg L/S ratios using a vacuum filtering system until a wastewater with a near neutral pH of 6–8 was achieved. The filtrate was then dried at 105 °C to a constant weight. The acid treatment procedure is shown in Fig. 1.

2.3. Characterisation methods

To determine the mineralogy, <2 μm clay fraction samples were prepared for XRD analysis by centrifugation following the protocol that has been previously described [16]. These were subjected to ethylene vapour treatment at 60 °C for 8 h and heat treatment at 400 °C for 1 h to aid clay mineral identification. Fig. 2 shows the XRD analysis of the resulting clay samples. The expansion of the (001) reflection from 14.7 Å to around 16.2 Å followed by its collapse at 400 °C confirmed the smectitic nature of the clay sample [17].

XRD Rietveld analysis was used to quantify the clay mineral phases and follow the acid activation in terms of the amorphous content of the output solid. The amorphous content (W_{AAM}) was measured using an internal standard method [18] by spiking the samples with 50 wt% Al$_2$O$_3$ (APC pure, UK) using the following formula:

$$W_{AM} = \frac{1 - W_{IS}^a / W_{IS}}{100 - W_{IS}^a} \times 10^4 \qquad (1)$$

where (W_{IS}^a) is the actual weighed amount of the internal standard material in the mix and (W_{IS}) is the weight percentage of the internal standard determined from Rietveld refinement [19]. XRD data was

Table 3
Acid activation treatment conditions.

Sample	Treatment duration	Temperature °C	Activating agent
1D	1 day	20	HCl 5 M
7D	7 days	20	HCl 5 M
21D	21 days	20	HCl 5 M
1H90	1 h	90	HCl 5 M
1HC90	1 h	90	HCl concentrated.
8H90	8 h	90	HCl 5 M

Table 2
XRD Rietveld analysis of the CEM I 52.5N Portland cement.

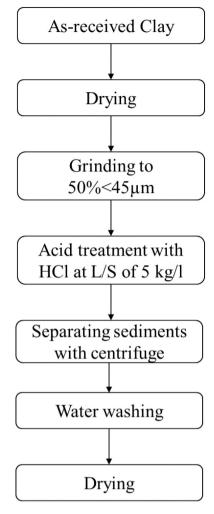| Phase name	Chemical formula	Quantity %	Space group	Lattice parameters					
				a	b	c	α	β	γ
Alite	Ca$_3$SiO$_5$	63.0	C1m1	12.24	7.08	9.30	–	116.11	–
Belite β	Ca$_2$SiO$_4$	13.4	P2$_1$/n	5.52	6.78	9.33	–	94.37	–
C3A cubic	Ca$_3$Al$_2$O$_6$	8.4	Pa-3	15.25	–	–	–	–	–
Brownmillerite	Ca$_2$Al$_{0.55}$Fe$_{1.45}$O$_5$	10.7	I2mb	5.34	14.62	5.53	–	–	–
Anhydrite	CaSO$_4$	2.6	Amma	7.00	7.02	6.24	–	–	–
Portlandite	Ca(OH)$_2$	1.9	P-3 m1	3.58	–	4.90	–	–	–

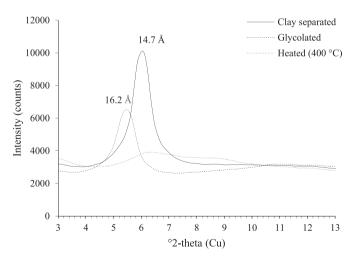**Fig. 1.** Acid activation procedure.

Fig. 2. XRD analysis of the clay fraction of the smectite sample showing a shift in (001) reflection to lower d-spacing after treatment with ethylene glycol and its collapse after heating at 400 °C.

recorded using a Rigaku Miniflex diffractometer with a Bragg-Brentano focusing geometry using Cu-Kα radiation ($\lambda = 1.5418$ Å) at 40 kV and 15 mA in the 2θ range of 3° to 45° with the scanning speed of 2°(2θ)/min and step size of 0.02°2θ. Samples were rotated at 10 rpm. The Rietveld refinement was performed using PDXL 2.8.4 software. Changes in chemical composition of clay particles were determined using SEM with EDS (JEOL JSM-6460 equipped with an Oxford Instruments Xplore EDS detector with 15 mm^2 sensor size). The specimens were mounted by sprinkling the clay particles onto double-sided carbon tape on a SEM stub and then coated with a conductive layer of carbon. EDS data were acquired at 20 kV accelerating voltage and a working distance of 8.5 mm.

FTIR spectroscopy was used to study modifications in the clay mineral structure subjected to acid dissolution. The IR spectra were recorded on a Bruker Alpha P FTIR spectrometer with platinum ATR (Attenuated Total Reflection) in the range of 4000–400 cm^{-1} by 32 scans at the spectral resolution of 4 cm^{-1}. The data was processed and analysed using OPUS software.

2.4. Assessment of pozzolanic activity

The pozzolanic activity of the AAS clay samples was assessed by a direct method using a modified Chapelle test [20]. The total quantity of $Ca(OH)_2$ fixed by the pozzolan was measured according to the method described in BS 8615-2:2019. 1 g of AAS clay and 2 g of CaO were added to an Erlenmeyer flask containing 250 ml distilled water. CaO was prepared by heating $CaCO_3$ (Sigma Aldrich) to 1000 °C for 1 h. The flask was connected to a condenser and kept at 85 °C for 16 h while being continually stirred. The flask content was then mixed with 250 ml of sucrose solution for 15 min and filtered (Whatman 42, 2.5 μm nominal pore size) and the filtrate then titrated against 0.1 N HCl using phenolphthalein as indicator. The total quantity of fixed $Ca(OH)_2$ in mg was calculated using:

$$mg\ Ca(OH)_2 = 2 \times \frac{V_1 - V_2}{V_1} \times \frac{74}{56} \times 1000 \qquad (2)$$

where V_1 and V_2 are the volume (ml) of HCl at the endpoint of titration of the blank and test samples respectively.

The effect of AAS clay in cement paste in terms of its ability to react with $Ca(OH)_2$ and on the hydration products was followed by XRD. PC blends with 25 wt% AAS at w/b ratio of 0.5 were prepared and stored in sealed 20 ml plastic containers at 20 °C for 28 days. Hydration was stopped using solvent exchange with isopropanol [21] and the solvent was replaced every 24 h for 3 days, followed by another 3 days drying in a vacuum desiccator. The samples were then ground using a McCrone mill prior to XRD analysis.

2.5. Mortar compressive strength

Mortar prisms of 160 × 40 × 40 mm with 25 % AAS clay as PC substitution at binder to sand ratio of 1:3 and water to binder ratio of 0.5 were prepared according to BS EN 196-1. The compressive strength of prisms halves were determined after 28 days of curing in water and compared with 100 % PC and 75 % PC:25 % PFA at the same age. Particle size distribution of the PC, PFA and AAS clay samples used in mortar strength testing was determined using a Mastersizer 2000 laser granulometer (Malvern Instruments) with a Scirocco 2000 dry dispersion unit. Fig. 9 shows the particle size distribution of PC, PFA and the 8H90 AAS clay sample.

3. Results

3.1. Characterisation of AAS

3.1.1. XRD

Fig. 3 shows the XRD data of the smectite clay sample subjected to acid treatment. Increasing the duration of the acid treatment at 20 °C from 1 day to 21 days had little effect on structural distortion of the smectite clay. When the treatment was performed at 90 °C the effect of
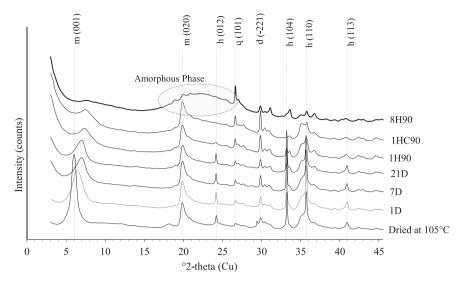
Fig. 3. XRD analysis of the smectite clay sample subjected to acid activation treatments showing a gradual dissolution of montmorillonite (001) basal plane and formation of an amorphous phase appearing as the "hump" in the region of between 20 and 30°2 theta. The identified peaks were m: montmorillonite, h: hematite, q: quartz and d: diopside.
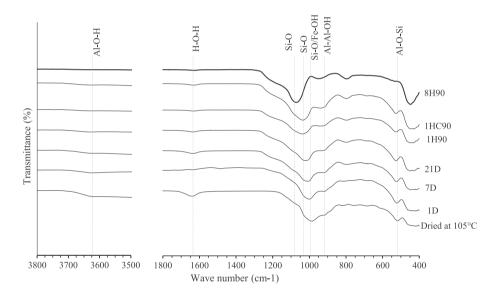

Fig. 4. FTIR analysis of AAS showing a shift in Si–O stretching band to higher wave numbers attributed to vibrations of amorphous silica with a three-dimensional framework.

increasing the activation time from 1 h to 8 h was more pronounced. The data shows that as the intensity of the acid treatment increases the d spacing of (001) basal reflection shifts from 14.7 Å (6.04 2°(2θ)) in the raw sample to around 11.5 Å (7.70 2°(2θ)). This can be attributed to leaching of the interlayer cations (Ca^{2+} and Mg^{2+}) and partial protonation of interlayer space [11]. The intensity of the (001) reflection also reduced with acid treatment and completely collapsed in the 8H90 sample. The complete disappearance of the clay basal and prismatic reflections in this sample was accompanied by the formation of an amorphous phase in the region of 20–30°2-θ [22]. This is related to the dissolution of the octahedral sheets and the subsequent release of the structural cations [23,24]. The intensity of (020) reflection remained unaltered in acid activated clays because structural changes occurred predominantly in the interlayers affecting basal rather that prismatic planes. Protons can attack the octahedral sheet at the edge of the layer or deplete cations in the interlayer through ion exchange [25]. This mechanism exposes the tetrahedral layer and initiates the deposition of amorphous silica as indicated by the formation of an amorphous 'hump'

in the XRD data. The diffraction attributed to impurities such as quartz became more apparent in acid activate clays, however some quartz and diopside were precipitated while hematite peaks weakened with increasing treatment intensity.

3.1.2. FTIR

Fig. 4 shows the FTIR spectra of AAS samples. The –OH stretching region in the raw as-received sample only shows a weak band at 1635 cm^{-1}, associated to the –OH stretching modes of Al(OH)Si groups, [26]. It was observed that the –OH band weakened in 1D sample and disappeared in 8H90 due to the leaching of octahedral cations Al^{3+} and Mg^{3+}, and protons penetrating into the smectite layers attacking the structural OH groups [24]. The depletion of iron from the octahedral sheet can be assigned to the disappearance of the vibration band at 993 cm^{-1} however, this overlaps with changes in vibrations of montmorillonite and therefore not very well resolved [27]. Changes in the structure of tetrahedral sheets were reflected in the shift in Si–O stretching band at around 1033 cm^{-1} to a new position close to 1083 cm^{-1}. The
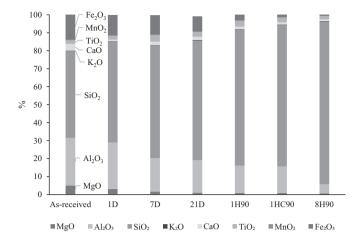
Fig. 5. EDS chemical composition of AAS samples calculated as the averaged of approximately 100 spectra acquired from the surface of clay particles. The data was normalised to 100 %.

appearance of absorption bands near 1080 and 800 cm^{-1} have been attributed to Si–O vibrations of amorphous silica with a three-dimensional framework [28]. The decrease in the intensity of (H–O–H) bending vibrations of water molecules at 1635 cm^{-1} and (Al–Al–OH) of octahedral Al in montmorillonite at 916 cm^{-1} also indicated the decomposition of smectite mineral structure with the increase in the acid treatment intensity [29].

3.1.3. SEM/EDS

Fig. 5 shows the chemical composition of AAS samples obtained from SEM/EDS analysis. The data was averaged from approximately 100 spectra acquired from the surface of clay particles as shown in Fig. 6 and presented as normalised oxide wt%. The results showed decreasing trends in the concentrations of MgO and Al_2O_3 with increase in acid activation intensity. The highest dissolution of cations was measured in 8H90 sample, where the concentration of MgO and Al_2O_3 dropped by 86 % and 81 % respectively. This confirms that the leaching of interlayer cations causes the structural changes in the octahedral sheets observed in the XRD and FTIR analyses. The increase in the cation dissolution rate resulted in the 8H90 clay particles being composed of 91 % SiO_2. This observation also confirmed the silica-based nature of the amorphous phase formed. EDS analysis confirmed the removal of calcite and hematite impurities in treated samples, while the concentration of TiO_2 remained unchanged. No trace of residual chloride in AAS samples was detected. SEM images showed no significant morphological changes in clay particles after the acid treatment.

3.2. Pozzolanic activity

Fig. 7 shows the results of the pozzolanic activity test as mg $Ca(OH)_2$ bound per mg AAS plotted against the amorphous content measured by the XRD Rietveld internal standard method. It was observed that AAS samples showed some pozzolanic activity even after mild acid treatment. All the treated samples exhibited ≥600 mg/g pozzolanic activity, the BS 8615–2 requirement for high reactivity natural calcined pozzolana for use in combination with PC. The data reveals correlation between the pozzolanic activity, and the amorphous content generated due to the acid activation. The highest pozzolanic activity of 1117 mg/g and the highest amorphous content of 93 % were measured in sample 8H90. Calcining the same sample of smectite clay at 850 °C produced a lower pozzolanic activity (369.6 mg/g). The calcined sample had 70 % amorphous content indicating that the amorphous phase generated during the calcining process may have a different structure and thus reactivity compared to those generated during acid activation.

3.3. XRD analysis of blended PC

Fig. 8a–c shows the XRD analysis of hydrated PC pastes with 25 % AAS clay after 28 days. The distinct peak of ettringite (Ett) at 9.1°2θ was visible in all the samples (Fig. 8a). The intensity of ettringite peak increased with the extent of acid activation. From the carboaluminate phases, hemicarboaluminate (Hc) was observed to be more stable in pastes with clays treated at lower activation intensities (1D, 7D and 21D), while monocarboaluminate (Mc) was dominant in clays treated at higher intensity (1H90C and 8H90). It must be noted that unlike
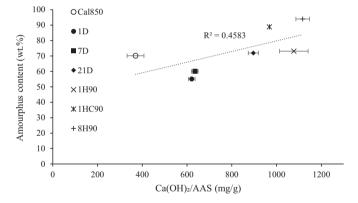

Fig. 7. The amorphous content generated during acid activation treatment and calcining at 850 °C (Cal850) plotted against pozzolanic activity test reported as mg $Ca(OH)_2$ bound per g AAS.
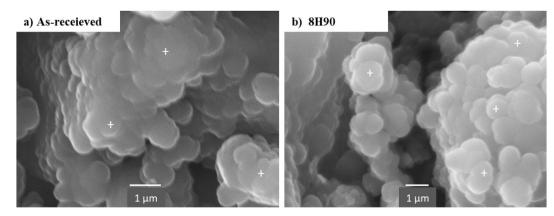

Fig. 6. SEM micrographs of (a) as received smectite clay showing typical positions of EDS spectra, and (b) AAS subjected to 8 hour treatment in 5 M HCl at 90 °C showing no significant detectable change in the clay morphology.
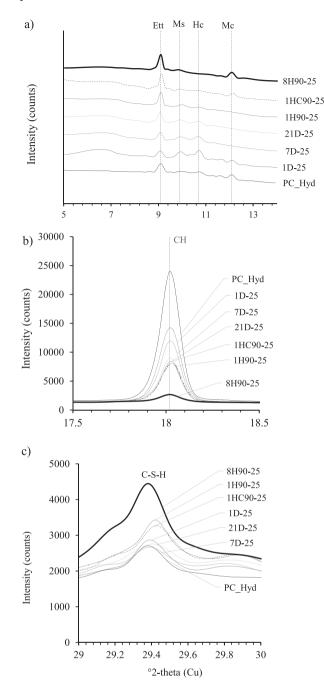
a)

b)

c)

Fig. 8. XRD patterns at 28 days of hydration for reference PC and 25 % AAS blends a) Ett: ettringite, Ms: monosulphoaluminate, Mc: monocarboaluminate, Hc: hemicarboaluminate, b) CH: portlandite and c) C-S-H gel.

Fig. 9. Particle size distribution of PC, PFA and 8H90 AAS sample.

Fig. 10. Compressive strength at 28 days of PC mortar prisms with 25 % PFA and AAS subjected to 8 hour treatment in 5 M HCl at 90 °C. Error bars show 95 % confidence interval.

calcined clays, AAS clays do not directly contribute to the formation of AFm and Aft phases in blended systems because AAS clay cannot supply extra alumina from pozzolanic reactions [30,31]. The pozzolanic reaction of AAS clays and portlandite (CH) in blended systems was investigated by XRD analysis as shown in Fig. 8b. It was evident that CH consumption increased in the presence of clays subjected to a more extensive acid treatment. The intensity of the CH peaks decreased drastically in the paste sample containing 25 % 8H90 AAS indicating a strong pozzolanic activity after 28 days hydration. The consumption of CH in pastes was accompanied by an increase in the intensity of C-S-H peaks as shown in Fig. 8c. This indicates that the amorphous content in AAS clays was responsible for the pozzolanic reactions because otherwise it would have diluted the system and caused a decrease in the intensity of the C-S-H phase.
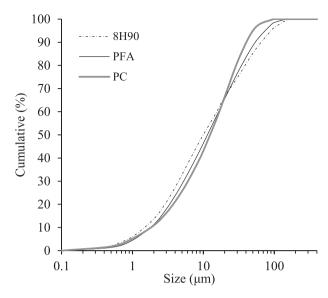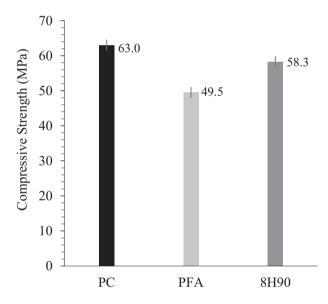
3.4. Compressive strength of mortar with AAS

To investigate the contribution of hydrated AAS clays to the compressive strength of cementitious systems, prisms with PC and 25 % 8H90 (the sample with highest pozzolanic activity) were prepared. These were compared to 100 % PC and PC with 25 % PFA.

The mean particle size of all three components was in a close range as shown in Fig. 9. Fig. 10 shows the compressive strength data. Mortar prisms with 25 % 8H90 AAS clay produced a compressive strength of 58.3 MPa. This was below the strength of plain PC mortar (63.0 MPa) but higher than those measured for cubes containing 25 % PFA (49.5 MPa).

4. Discussions

Acid activation of smectite clay using HCl produced a significant amount of amorphous phase. All characterisation methods indicate a mechanism for acid activation involving protons entering the smectite layers, attacking the structural OH groups and leaching out the exchangeable hydrated cations. The resulting dehydroxylation gradually released the central atoms from the octahedral site and this transforms the tetrahedral sheets to a three-dimensional silica based amorphous phase, the amount of which was closely related to the intensity of acid activation in terms of duration and temperature. The formation of the amorphous phase has been reported to increase the structural porosity [32]. This can provide additional surface for nucleation during the early hydration stages and contribute to the compressive strength of the blended systems.

The amorphous phase formed by acid activation treatment had a higher pozzolanic activity compared to that formed during calcining treatment at 850 °C. Attention must be paid when associating the pozzolanic activity measured as the consumption of $Ca(OH)_2$ to the exact performance in a blended system. This is because protonated sites in the structure of AAS clays can absorb Ca^{2+} ions and cause overestimation of the pozzolanic activity [33]. However, there was strong evidence that the amorphous phase formed in AAS clays contributed to the formation of C-S-H and compressive strength development.

The intrinsic reactivity of the amorphous phase is mainly determined by the chemical composition and the degree of polymerisation [34]. This is the case for the glass phase generated at high temperature where the presence of alkali or earth alkali ions acting as network-modifying ions can disrupt the silica network and result in higher reactivities [35]. The reactivity of calcined smectite clay has been attributed to changes in the local environment of the Al atoms in the octahedral sheet due to the structural dehydroxylation [36]. A similar mechanism seems to be occurring in AAS clays and this explains the reactivity of the amorphous phase generated. However, further analysis of the amorphous phase structure is needed to describe the hydraulic and basicity properties of AAS clays.

The acid activation treatment for smectite clays may represent a low carbon alternative to high temperature calcining treatment for producing supplementary cementitious materials. The findings of this study show the potential for acid activation to produce a pozzolanic material with a higher reactivity compared to its calcined from. HCl is relatively cheap (USD 145/MT - chemanalyst.com) and vastly available in Western Europe (5.7 million tonnes per annum), either from direct synthesis or as a by-product of other chemical engineering processes such as vinyl chloride and polyurethane production [37]. However, HCl is a strong highly corrosive acid, and this represents a drawback compared to the calcining technology. The highest reactivity was observed in sample 8H90 which was subjected to 8 h of acid treatment. This also compares unfavourably to calcining where the treatments are usually conducted in <1 h [38]. The use of 5 M HCl is the greatest contributor to embodied carbon in this sample. The treatment at lower acid/solid ratios and multiple recycling of the reagent could reduce the embodied carbon to below that for calcined clays (0.26 kg CO_2eq – Ecoinvent version 3.7.1).

This research has demonstrated the potential for AAS clays to be used as reactive pozzolans. Acid activated clays have been extensively used as catalysts with many industrial applications. However, their use as SCMs has not previously been reported prior to this work. Optimisation of various aspects of the technology is of outmost importance. Further research is required to fine tune the treatment process and better understand the structure and hydration mechanisms of AAS clays. This would allow the incorporation of AAS clays in cementitious systems at higher substitution levels and production of pozzolanic materials by activating other types of clay minerals.

5. Conclusions

This research has shown, for the first time, that treating smectite clay with strong acid generates a material with pozzolanic activity. It was found that acid treatment causes dehydroxylation reaction followed by the leaching of exchangeable cations and Al from octahedral sheets producing a reactive silica based amorphous phase. The AAS clays exhibited a higher pozzolanic activity compared to calcined smectite. Activating the smectite sample with 5 M HCl for 8 h at 90 °C generated 93 % amorphous phase with clay particles composed of 91 % silica and 1117 mg/g pozzolanic activity. The performance of the optimally acid activated smectite in PC paste revealed a near complete consumption of portlandite, and formation of additional C-S-H phase. Mortars with 25 % substitution level of acid activated smectite clay achieved compressive strengths of 58.3 MPa compared 63.0 MPa produced using 100 % PC. The results demonstrate the capability of acid treatment to provide a new generation of potentially low-carbon supplementary cementitious materials to the construction sector. Further understanding of activated clay mineral structure and optimisation of the treatment process are needed.

Declaration of competing interest

The authors declare that they have no known competing financial interests or personal relationships that could have appeared to influence the work reported in this paper.

Data availability

Data will be made available on request.

Acknowledgments

References

[1] G. Yao, H. Zang, J. Wang, P. Wu, J. Qiu, X. Lyu, Effect of mechanical activation on the pozzolanic activity of muscovite, Clay Clay Miner. 67 (3) (2019) 209–216.

[2] B. Ilić, V. Radonjanin, M. Malešev, M. Zdujić, A. Mitrović, Effects of mechanical and thermal activation on pozzolanic activity of kaolin containing mica, Available from, Appl. Clay Sci. 123 (2016) 173–181, https://www.sciencedirect.com/science/article/pii/S0169131716300230.

[3] M. Fitos, E.G. Badogiannis, S.G. Tsivilis, M. Perraki, Pozzolanic activity of thermally and mechanically treated kaolins of hydrothermal origin, Available from, Appl. Clay Sci. 116–117 (2015) 182–192, https://www.sciencedirect.com/science/article/pii/S0169131715300922.

[4] N.S. Msinjili, G.J.G. Gluth, P. Sturm, N. Vogler, H.C. Kühne, Comparison of calcined illitic clays (brick clays) and low-grade kaolinitic clays as supplementary cementitious materials, Mater. Struct. 52 (5) (2019) 94, https://doi.org/10.1617/s11527-019-1393-2. Available from:.

[5] D. Zhou, R. Wang, M. Tyrer, H. Wong, C. Cheeseman, Sustainable infrastructure development through use of calcined excavated waste clay as a supplementary cementitious material, J. Clean. Prod. 168 (2017) 1180–1192.

[6] I. Tkáč, P. Komadel, D. Müller, Acid-treated Montmorillonites—a study by 29 si and 27 Al MAS NMR, Available from: Clay Miner. 29 (1) (1994) 11–19. Mar 9 [cited 2020 Mar 3, https://www.cambridge.org/core/product/identifier/S0009855800027163/type/journal_article.

[7] V. Krupskaya, L. Novikova, E. Tyupina, P. Belousov, O. Dorzhieva, S. Zakusin, et al., The influence of acid modification on the structure of montmorillonites and surface properties of bentonites, May 1 [cited 2020 Mar 5], Appl. Clay Sci. 172 (2019) 1–10. Available from: https://www.sciencedirect.com/science/article/pii/S0169131719300316?via%3Dihub.

[8] P. Komadel, J. Madejová, Chapter 7.1 acid activation of clay minerals, Available from: Dev. Clay Sci. 1 (2006 Jan 1) 263–287 https://www.sciencedirect.com/science/article/pii/S1572435205010081.

[9] A. Steudel, L.F. Batenburg, H.R. Fischer, P.G. Weidler, K. Emmerich, Alteration of non-swelling clay minerals and magadiite by acid activation, Available from: Appl. Clay Sci. 44 (1–2) (2009) 95–104. Apr 1 [cited 2020 Mar 5, https://www.sciencedirect.com/science/article/pii/S0169131709000301?via%3Dihub.

[10] C.N. Rhodes, D.R. Brown, Catalytic activity of acid-treated montmorillonite in polar and non-polar reaction media, Catal. Lett. 24 (3) (1994) 285–291.

[11] V.V. Krupskaya, S.V. Zakusin, E.A. Tyupina, O.V. Dorzhieva, A.P. Zhukhlistov, M. N. Timofeeva, Experimental study of montmorillonite structure and transformation of its properties under the treatment of inorganic acid solutions [cited 2020 Mar 12]; Available from: https://www.preprints.org/manuscript/201612.0100/v1, 2016 Dec 19.

[12] N. Jovanović, J. Janaćković, Pore structure and adsorption properties of an acid-activated bentonite, Available from, Appl. Clay Sci. 6 (1) (1991) 59–68, https://www.sciencedirect.com/science/article/pii/0169131791900107.

[13] R. Zhu, Q. Chen, Q. Zhou, Y. Xi, J. Zhu, H. He, Adsorbents based on montmorillonite for contaminant removal from water: a review, Apr 1 [cited 2020 Mar 4], Appl. Clay Sci. 123 (2016) 239–258. Available from: https://www.sciencedirect.com/science/article/pii/S0169131715302155.

[14] F. Gómez-Sanz, M.V. Morales-Vargas, B. González-Rodríguez, M.L. Rojas-Cervantes, E. Pérez-Mayoral, Acid clay minerals as eco-friendly and cheap catalysts for the synthesis of β-amino ketones by Mannich reaction, Jul 1 [cited 2020 Mar 4], Appl. Clay Sci. 143 (2017) 250–257. Available from: https://www.sciencedirect.com/science/article/pii/S0169131717301436.

[15] H.S. Ndé, P.A. Tamfuh, G. Clet, J. Vieillard, M.T. Mbognou, E.D. Woumfo, Comparison of HCl and H2SO4 for the acid activation of a cameroonian smectite soil clay: palm oil discolouration and landfill leachate treatment, Heliyon 5 (12) (2019), e02926. Available from: https://www.sciencedirect.com/science/article/pii/S2405844019365855.

[16] L.J. Poppe, V.F. Paskevich, J.C. Hathaway, D.S. Blackwood, A laboratory manual for X-ray powder diffraction, US Geol. Surv. Open-File Rep. 1 (041) (2001) 1–88.

[17] D.M. Moore, R.C. Reynolds Jr., X-ray Diffraction and the Identification and Analysis of Clay Minerals, Oxford University Press, OUP, 1989.

[18] I.C. Madsen, N.V.Y. Scarlett, A. Kern, Description and survey of methodologies for the determination of amorphous content via X-ray powder diffraction, Z. Krist. Cryst. Mater. 226 (12) (2011) 944–955.

[19] Y.P. Stetsko, N. Shanahan, H. Deford, A. Zayed, Quantification of supplementary cementitious content in blended Portland cement using an iterative Rietveld–PONKCS technique, J. Appl. Crystallogr. 50 (2) (2017) 498–507, https://doi.org/10.1107/S1600576717002965. Available from:.

[20] E. Ferraz, S. Andrejkovicova, W. Hajjaji, A.L. Velosa, A.S. Silva, F. Rocha, Pozzolanic activity of metakaolins by the french standard of the modified chapelle test: a direct methology, Acta Geodyn Geomater. 12 (3) (2015) 289–298.

[21] K. Scrivener, R. Snellings, B. Lothenbach, A Practical Guide to Microstructural Analysis of Cementitious Materials Vol. 540, Crc Press, Boca Raton, 2016.

[22] M. Pentrák, V. Hronský, H. Pálková, P. Uhlík, P. Komadel, J. Madejová, Alteration of fine fraction of bentonite from kopernica (Slovakia) under acid treatment: a combined XRD, FTIR, MAS NMR and AES study, Oct 1 [cited 2020 Mar 3], Appl. Clay Sci. 163 (2018) 204–213. Available from: https://www.sciencedirect.com/science/article/pii/S016913171830334X?via%3Dihub.

[23] G.E. Christidis, P.W. Scott, A.C. Dunham, Acid activation and bleaching capacity of bentonites from the islands of Milos and Chios, Aegean, Greece, Available from, Appl. Clay Sci. 12 (4) (1997) 329–347, http://www.sciencedirect.com/science/article/pii/S0169131797000173.

[24] K. Al-Essa, Activation of jordanian bentonite by hydrochloric acid and its potential for olive mill wastewater enhanced treatment, J Chem. 2018 (2018).

[25] F. Franco, M. Pozo, J.A. Cecilia, M. Benítez-Guerrero, M. Lorente, Effectiveness of microwave assisted acid treatment on dioctahedral and trioctahedral smectites. The influence of octahedral composition, Available from: Appl. Clay Sci. 120 (2016) 70–80 https://www.sciencedirect.com/science/article/pii/S016913171530185X.

[26] J.A. Cecilia, L. Pardo, M. Pozo, E. Bellido, F. Franco, Microwave-assisted acid activation of clays composed of 2:1 clay minerals: a comparative study, Minerals 8 (2018).

[27] P. Yuan, F. Annabi-Bergaya, Q. Tao, M. Fan, Z. Liu, J. Zhu, et al., A combined study by XRD, FTIR, TG and HRTEM on the structure of delaminated fe-intercalated/pillared clay, Available from, J. Colloid Interface Sci. 324 (1) (2008) 142–149, http://www.sciencedirect.com/science/article/pii/S002197970800547X.

[28] J. Madejová, FTIR techniques in clay mineral studies, Available from, Vib. Spectrosc. 31 (1) (2003) 1–10, http://www.sciencedirect.com/science/article/pii/S0924203102000656.

[29] A. Amari, H. Gannouni, M.I. Khan, M.K. Almesfer, A.M. Elkhaleefa, A. Gannouni, Effect of structure and chemical activation on the adsorption properties of green clay minerals for the removal of cationic dye, Appl. Sci. 8 (11) (2018) 2302.

[30] M. Antoni, J. Rossen, F. Martirena, K. Scrivener, Cement substitution by a combination of metakaolin and limestone, Available from, Cem. Concr. Res. 42 (12) (2012) 1579–1589, https://www.sciencedirect.com/science/article/pii/S0008884612002074.

[31] W. Kunther, Z. Dai, J. Skibsted, Thermodynamic modeling of Portland cement—Metakaolin—Limestone blends, in: Calcined Clays for Sustainable Concrete, Springer, 2015, pp. 143–149.

[32] V.A.A. España, B. Sarkar, B. Biswas, R. Rusmin, R. Naidu, Environmental applications of thermally modified and acid activated clay minerals: current status of the art, Environ. Technol. Innov. 13 (2019) 383–397.

[33] S. Papatzani, E.G. Badogiannis, K. Paine, The pozzolanic properties of inorganic and organomodified nano-montmorillonite dispersions, Available from, Constr. Build. Mater. 167 (2018) 299–316, http://www.sciencedirect.com/science/article/pii/S0950061818301466.

[34] J. Skibsted, R. Snellings, Reactivity of supplementary cementitious materials (SCMs) in cement blends, Available from, Cem. Concr. Res. 124 (2019), 105799, https://www.sciencedirect.com/science/article/pii/S0008884619302327.

[35] M. Moesgaard, D. Herfort, J. Skibsted, Y. Yue, Calcium aluminosilicate glasses as supplementary cementitious materials, Glas. Technol. J. Glas. Sci. Technol. Part A 51 (5) (2010) 183–190.

[36] N. Garg, J. Skibsted, Pozzolanic reactivity of a calcined interstratified illite/smectite (70/30) clay, Available from, Cem. Concr. Res. 79 (2016) 101–111, https://www.sciencedirect.com/science/article/pii/S0008884615002288.

[37] H.J. Althaus, M. Chudacoff, R. Hischier, N. Jungbluth, M. Osses, A. Primas, Life cycle inventories of chemicals, Ecoinvent. Rep. 2 (2007).

[38] T. Hanein, K.C. Thienel, F. Zunino, A. Marsh, M. Maier, B. Wang, et al., Clay calcination technology: state-of-the-art review by the RILEM TC 282-CCL, Mater. Struct. 55 (1) (2022) 1–29.